OPEN

Journal of Cerebral Blood Flow & Metabolism (2014) 34, 389–396

www.jcbfm.com

ORIGINAL ARTICLE

Changes in cerebral blood flow during steady-state cycling exercise: a study using oxygen-15-labeled water with PET

Mikio Hiura[1,2], Tadashi Nariai[2,3], Kenji Ishii[2], Muneyuki Sakata[2], Keiichi Oda[2], Jun Toyohara[2] and Kiichi Ishiwata[2]

Cerebral blood flow (CBF) during dynamic exercise has never been examined quantitatively using positron emission tomography (PET). This study investigated changes in CBF that occur over the course of a moderate, steady-state cycling exercise. Global and regional CBF (gCBF and rCBF, respectively) were measured using oxygen-15-labeled water ($H_2{}^{15}O$) and PET in 10 healthy human subjects at rest (Rest), at the onset of exercise (Ex1) and at a later phase in the exercise (Ex2). At Ex1, gCBF was significantly ($P<0.01$) higher (27.9%) than at Rest, and rCBF was significantly higher than at Rest in the sensorimotor cortex for the bilateral legs ($M1_{Leg}$ and $S1_{Leg}$), supplementary motor area (SMA), cerebellar vermis, cerebellar hemispheres, and left insular cortex, with relative increases ranging from 37.6% to 70.5%. At Ex2, gCBF did not differ from Rest, and rCBF was significantly higher (25.9% to 39.7%) than at Rest in only the $M1_{Leg}$, $S1_{Leg}$, and vermis. The areas showing increased rCBF at Ex1 were consistent with the central command network and the anatomic pathway for interoceptive stimuli. Our results suggest that CBF increases at Ex1 in parallel with cardiovascular responses then recovers to the resting level as the steady-state exercise continues.

Journal of Cerebral Blood Flow & Metabolism (2014) **34,** 389–396; doi:10.1038/jcbfm.2013.220; published online 4 December 2013

Keywords: brain imaging; cerebral blood flow measurement; exercise; physiology; positron emission tomography

INTRODUCTION

Up to now, the mechanisms regulating cerebral blood flow (CBF) during exercise have been examined only in the context of the physiologic factors affecting cardiovascular control.[1–3] It has been shown, for example, that CBF increases by ~25% during moderate cycling exercise to volitional exhaustion, as compared with rest, unless there is a fall in the arterial CO_2 (P_aCO_2) tension.[4–6] Moreover, in these investigations, CBF was analyzed using transcranial Doppler ultrasound, mainly to detect the mean blood velocity in the middle cerebral artery. Consequently, neither the gCBF nor specific rCBFs were identified.

There have been several studies in which imaging using positron emission tomography (PET) or single-photon emission computed tomography (SPECT) was used to visualize changes in rCBF during moderate cycling exercise.[7–9] For this purpose, not only does PET enable quantitative analysis of gCBF, its spatial resolution also enables analysis of rCBF in discrete regions. Furthermore, it is widely believed that certain specific brain regions are involved in regulating the cardiovascular response to dynamic exercise; this has been termed 'the central command theory'.[10] For example, previous studies using PET or SPECT demonstrated that changes in rCBF in the insular cortex and anterior cingulate gyrus are associated with central command and are mainly related to autonomic adjustments during exercise.[8,9,11,12] With that in mind, we hypothesized that these regions might serve as the higher brain areas involved in autonomic adaptation during exercise. This regulatory system appears to be required specifically during the transient phase between rest and exercise, before the cardiovascular response reaches a state of equilibrium.

When moderate exercise continues at a constant workload, the cardiovascular response reaches a steady state in which the kinetics of pulmonary oxygen consumption ($\dot{V}O_2$) plateaus.[13] In addition, cardiac output (CO) increases during the exercise, and the increase in blood flow is thought to be distributed mainly to the working muscle, although the changes in rCBF over the course of steady-state exercise have never been investigated. Therefore, the purpose of the present study was to use oxygen-15-labeled water ($H_2{}^{15}O$) and PET to investigate the changes in rCBF that occur during the initial phase and a later phase of a moderate, steady-state cycling exercise. In addition, to relate changes in rCBF to cardiovascular responses during the exercise, physiologic variables were measured as well.

MATERIALS AND METHODS

Subjects

Ten young male volunteers (22.7 ± 1.9 years; mean height, 1.75 ± 0.05 m; mean body mass, 65.9 ± 9.8 kg) participated in the study. Each subject provided a detailed medical history to ensure that he was in good health and not taking any medication, and all of the subjects were found to be anatomically normal on magnetic resonance imaging (MRI), as described below. The subjects were instructed to live and eat as normally as possible, but to avoid rigorous exercise, alcohol, and drugs during the 24 hours preceding the experiments. All of the participants provided informed consent before entering in the study. The study protocol was governed by the guidelines of national government based on the Helsinki Declaration revised in 1983, and it was approved by the Ethics Committee of Tokyo Metropolitan Institute of Gerontology and was conducted at the Tokyo Metropolitan Institute of Gerontology.

Study Design and Monitoring

The study protocol is illustrated in Figure 1. Before the scan, subjects were trained in the experimental procedures, especially cycling on a supine

[1]Faculty of Sports and Health Studies, Hosei University, Tokyo, Japan; [2]Research Team for Neuroimaging, Tokyo Metropolitan Institute of Gerontology, Tokyo, Japan and [3]Department of Neurosurgery, Tokyo Medical and Dental University, Tokyo, Japan. Correspondence: Dr M Hiura, Faculty of Sports and Health Studies, Hosei University, 4342 Aihara-cho, Machida-shi, Tokyo 194-0298, Japan.
E-mail: phmikmd@hosei.ac.jp
This work was supported by a Grant-in Aid for Scientific Research (C) No. 24500478 from the Japan Society for the Promotion of Science (to Mikio Hiura).
Received 1 August 2013; revised 9 October 2013; accepted 11 November 2013; published online 4 December 2013

ergometer (Load, Groningen, the Netherlands). A week before the main study, the exercise intensity needed to drive the heart rate (HR) to 50% to 60% of the estimated maximum during the plateau phase of the exercise was determined for each subject. Maximum HR was estimated by subtracting the subject's age from 220. At this exercise intensity, the subjects were able to pedal without apparent movement of the head during the main experiment.

Subjects were placed on the scanner bed in the supine position with their heads immobilized in a customized head holder. Ambient noise was kept to a minimum, and the subjects kept their eyes open during all scans. Before the scans, a catheter was placed in the left radial artery to measure arterial time–activity curves as well as P_aCO_2. For injection of $H_2{}^{15}O$, a cannula was placed in the right cubital vein. The first PET scan (baseline measurements) was performed while the subjects were breathing room air at Rest. A cycling exercise at a constant workload was initiated 7 minutes later, and the second and third scans were performed 3 minutes (Ex1) and 13 minutes (Ex2) after the onset of the exercise. The interscan intervals were thus 10 minutes. The exercise was performed on the scanner bed using a supine positioned cycle ergometer. Each subject was instructed to pedal at a constant rate of 60 r.p.m. at the predetermined workload. Exercise was continued at a constant workload for 15 minutes.

An online gas analyzer (Cosmed, Rome, Italy) was used to measure VO_2 and several variables related to ventilation, including end-tidal partial pressure of CO_2. Cardiac output, HR, systolic blood pressure, and diastolic blood pressure were measured using an impedance cardiograph device (Manatec, Paris, France). Mean blood pressure (MBP) was calculated as follows: MBP = 1/3 * (2 diastolic blood pressure + systolic blood pressure). For all variables, data were sampled as the average over every 15 seconds. Arterial CO_2 was measured from arterial blood samples.

Image Sequence

The scans were performed using a SET2400W PET scanner (Shimadzu, Kyoto, Japan) operating in three-dimensional mode and producing 63 image slices with an interslice interval of 3.125 mm. The intrinsic spatial resolution was 4.4 mm in-plane and 6.4 mm full width at half-maximum axially. The data were reconstructed using a Butterworth filter (cut-off frequency, 1.25 cycles/cm; order, 2) with standard correction for attenuation and scatter. Before $H_2{}^{15}O$ administration, a 6-minute transmission scan was acquired using $^{68}Ga/^{68}Ge$ rotating rod sources for estimation of attenuation correction. Thereafter, 300 MBq $H_2{}^{15}O$ was intravenously injected into each subject as a bolus (over < 5 seconds), and an accumulated image was acquired for a total of 2 minutes after injection. At the same time as the PET emission data were being acquired, arterial blood was being continuously drawn, and the radioactivity level was monitored using a beta detector equipped with a plastic scintillator (Shimadzu, Kyoto, Japan). These data were then used in an input function to compute the CBF after correction for delay and dispersion. With the accumulated image and the measured arterial input function, the rCBF was calculated on a pixel-by-pixel basis using the autoradiographic method.[14,15] The 10-minute intervals between $H_2{}^{15}O$ injections were sufficient for decay of the radioactivity.

For anatomic reference, individual brain MRI scans were acquired on a separate occasion using a 1.5 Tesla Signa Excite HD scanner (General Electric, Milwaukee, WI, USA). Sagittal images were obtained with T1-weighted contrast (3DSPGR; TR = 9.2 milliseconds, TE = 2.0 milliseconds, matrix size = 256 × 256 × 124, voxel size = 0.94 × 0.94 × 1.3 mm) and T2-weighted contrast (first spin echo; TR = 3000 milliseconds, TE = 100 milliseconds, matrix size = 256 × 256 × 20, voxel size = 0.7 × 0.7 × 6.5 mm).

Image Processing and Analysis

The image data were analyzed using Statistical Parametric Mapping (SPM 8, Welcome Department, London, UK) software and Matlab 7.0 (MathWorks, Natick, MA, USA). Sequential PET images acquired during the activation in each subject were realigned, and the mean realigned image was co-registered to individual MRIs and then projected into a standard three-dimensional stereotactic space using the SPM 8 and the MNI (Montreal Neurological Institute) templates, sampled at a voxel size of 2 × 2 × 2 mm. And for the quantitative analysis of rCBF described below, individual MRIs were spatially normalized so that they would have the same anatomic space as the PET images. The spatially normalized images of all subjects were smoothed using an isotropic Gaussian filter (full-width half-maximum 12 mm).

Voxel-based SPM analyses were performed without global normalization—i.e., using absolute rCBF values. Data were analyzed using two statistical models. A design matrix of subject-by-task interactions was constructed to test exercise-induced changes in rCBF between conditions: Rest versus Ex1 and Rest versus Ex2 (paired *t*-test). Initially, regions comprising the entire brain volume with corrected significance level of $P < 0.05$ were explored. We then accepted uncorrected significance levels of $P < 0.001$, which corresponded to Z-scores > 3.09 (i.e., voxel levels of significance uncorrected for multiple analyses over the whole brain). We examined for tendency by rerunning the same analysis at a level of $P < 0.01$, which corresponded to Z-scores > 2.33. In addition, a small volume correction factor was applied to areas of increased rCBF hypothesized based on earlier findings to be involved in the execution of exercise, or central command.[8,9,11,12] Significant increases or decreases are reported for clusters greater than 30 voxels in size.

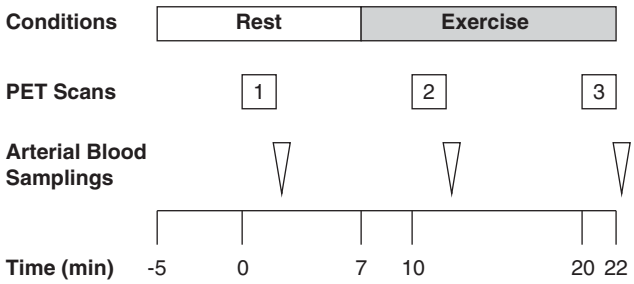

Figure 1. Diagram of the experimental protocol used for acquisition of oxygen-15-labeled water ($H_2{}^{15}O$) positron emission tomography (PET) and arterial blood samples. Injection time of $H_2{}^{15}O$ for the first PET scan was defined as Time 0.

The quantitative analysis of rCBF was performed using Dr View software (Infocom, Tokyo, Japan) based on the results from the SPM analysis. We then distributed circular regions of interest (ROIs; 10 mm in diameter) in areas where rCBF was significantly higher at Ex1 than at Rest. In addition, ROIs were selected within the right and left insular cortex, because earlier studies identified a lateralized functionality related to autonomic control within the insular cortices.[8,16,17]The ROIs were drawn on an averaged MRI from the each subject's PET–MRI co-registered and normalized image, which was then resliced into 5-mm thicknesses (Figure 2). To determine rCBF, the normalized PET images were co-registered to the 5-mm-thick averaged MRI, and the average rCBF values within the individual ROIs were calculated from the corresponding 5-mm-thick PET images using Dr View software. Furthermore, gCBF was defined using the segmentation strategy included in Dr View software using a threshold derived from the bitmap.

Values are expressed as means ± s.d. ($n = 10$). For physiologic variables and quantitative rCBF data obtained from ROI-based analysis, comparisons among the three conditions were made using repeated measures one-way analysis of variance with activation (Rest, Ex1, and Ex2) as a within-factor. If significant F-ratios were detected, Turkey's *post hoc* test was applied. All analyses were carried out using GraphPad Prism 6.0 (GraphPad, San Diego, CA, USA). For physiologic variables obtained during each 2-minute PET scan, comparisons of the eight 15-second sampling bins were also made using repeated measures one-way analysis of variance.

RESULTS

Physiologic Data Analysis

During the cycle ergometer exercise, the average workload was 71 ± 11 watts. The time course of the changes in physiologic parameters is shown in Figure 3A. None of the parameters changed significantly during the 2-minute periods required for each PET scan (repeated measures one-way analysis of variance). With the exception of MBP, which was consistently measured at 86 to 87 mm Hg, all of the parameter values measured at Ex1 and Ex2 differed significantly from those at Rest (Table 1). Because we used a steady-state exercise model, there were no differences between HR and VO_2 at Ex1 and Ex2, with HR ranging from 96 to 104 b.p.m. and VO_2 ranging from 18.6 to 18.8 mL/kg per minute. Cardiac output increased sharply to 7.3 L/minute at Ex1 and then gradually increased to 8.3 L/minute by Ex2. Both end-tidal partial pressure of CO_2 and P_aCO_2 were significantly higher at Ex1 and Ex2 than at Rest, but there was no difference between Ex1 and Ex2, despite individual differences in the patterns of change in

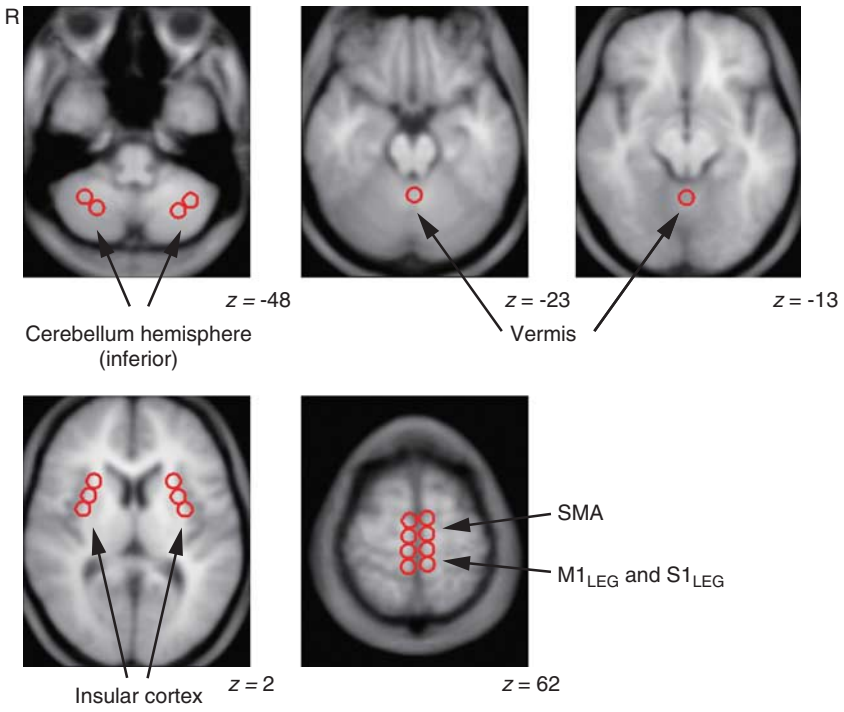

Figure 2. Representative images showing distributed regions of interest. Multiple circular areas, 10 mm in diameter, were placed on the magnetic resonance imaging (MRI) averaged from 10 images from each subject's co-registered positron emission tomography –MRI image, which was resliced at a thickness of 5 mm. The Montreal Neurological Institute coordinate in the *z* dimension is given for each slice. *R* indicates right side of the brain. $M1_{Leg}$, primary motor cortex for legs; SMA, supplementary motor cortex; $S1_{Leg}$, primary sensory cortex for legs.

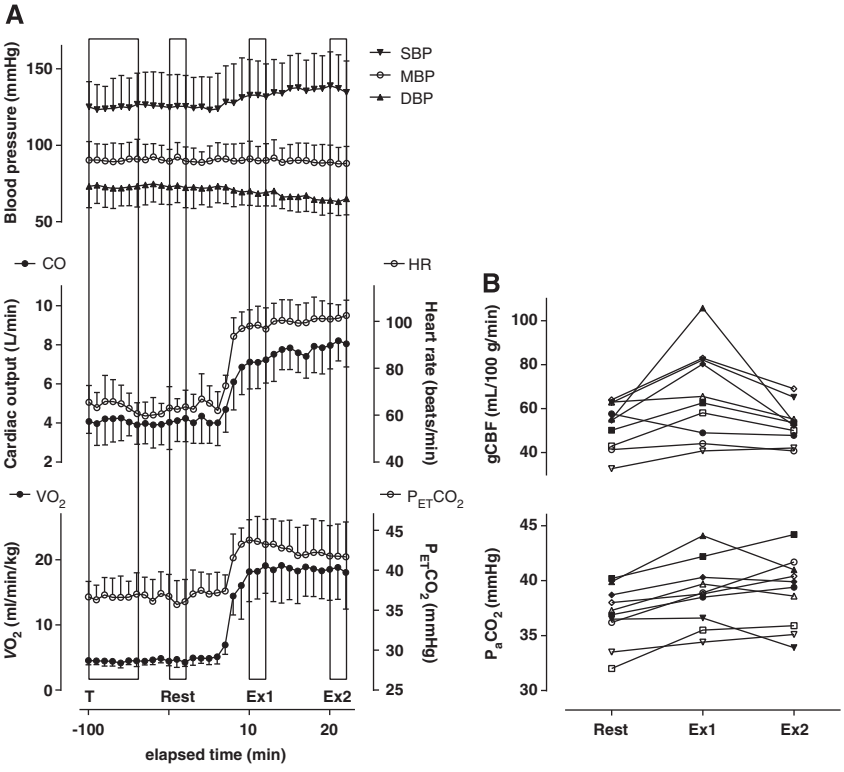

Figure 3. Changes in the indicated physiologic parameters and quantitative gCBF during moderate, steady-state cycling exercise. (**A**) Time course of the indicated physiologic parameters. Boxes indicate the transmission scan (T), emission scans of the Rest, Ex1, and Ex2 periods. Injection time of oxygen-15-labeled water for the first positron emission tomography (PET) scan was defined as Time 0. Each data point represents the mean ± s.d. of a 1-minute epoch ($n = 10$). (**B**) Individual results for arterial CO_2 (P_aCO_2) and global cerebral blood flow (gCBF) at Rest, Ex1, and Ex2. Each symbol represents an individual subject. DBP, diastolic blood pressure; HR, heart rate; MBP, mean blood pressure; SBP, systolic blood pressure; VO_2, pulmonary oxygen consumption.

Table 1. Physiologic parameters measured at Rest and during exercise

	Rest	*Ex1*	*Ex2*
Heart rate (b.p.m.)	60 ± 5	96 ± 2***	104 ± 9***
Cardiac output (L/minute)	3.8 ± 0.7	7.3 ± 1.4***	8.3 ± 1.5***†
VO_2 (mL/min per kg)	5.4 ± 1.2	18.6 ± 4.4***	18.8 ± 4.2***
Systolic blood pressure (mm Hg)	123 ± 20	133 ± 22*	135 ± 20**
Diastolic blood pressure (mm Hg)	74 ± 13	68 ± 9	64 ± 9*
Mean blood pressure (mm Hg)	86 ± 14	87 ± 9.4	86 ± 10
$P_{ET}CO_2$ (mm Hg)	37.1 ± 2.1	43.9 ± 3.8***	42.2 ± 4.0***
P_aCO_2 (mm Hg)	36.9 ± 2.6	38.9 ± 2.9**	39.0 ± 3.2*

P_aCO_2, arterial tension of carbon dioxide; $P_{ET}CO_2$, end-tidal partial pressure of carbon dioxide; VO_2, pulmonary oxygen uptake. Values are shown as means ± s.d. ($n = 10$). With the exception of P_aCO_2, the data were averaged over 2 minutes of the PET scan. Significance of difference from Rest: *$P<0.05$, **$P<0.01$, ***$P<0.0001$. Significance of difference from Ex1: †$P<0.05$.

P_aCO_2 between Ex1 and Ex2 (Figure 3B). Moreover, the changes in end-tidal partial pressure of CO_2 during exercise were larger than the changes in P_aCO_2 (5 to 6 mm Hg versus 2 mm Hg), which is consistent with the P_aCO_2–end-tidal partial pressure of CO_2 relationship seen during exercise by Jones *et al.*[18] For further analysis, we selected P_aCO_2 as one of the factors contributing to the regulation of exercise-related changes in CBF.

Statistical Parametric Mapping Analysis

As shown in Table 2 and Figure 4, rCBF was higher in the cerebellar vermis and sensorimotor cortex for the bilateral legs ($M1_{Leg}$ and $S1_{Leg}$) at Ex1 ($P<0.05$, corrected) than at Rest. There were also significant increases in rCBF in the bilateral supplementary motor area (SMA), bilateral inferior cerebellar hemispheres and left insula cortex at Ex1 ($P<0.001$, uncorrected). No reductions in rCBF were observed at Ex1, as compared with Rest ($P<0.01$, uncorrected). At Ex2, rCBF in the vermis was significantly higher than at Rest ($P<0.05$, corrected). There were also significant increases in rCBF in $M1_{Leg}$, $S1_{Leg}$, and the SMA at Ex2 ($P<0.001$, uncorrected). However, the sizes of the areas showing an elevation in rCBF were smaller at Ex2 than Ex1. In particular, the increase in rCBF in the SMA was confined to a very small area at Ex2. No reductions in rCBF were observed at Ex2, as compared with Rest ($P<0.001$, uncorrected). However, there was a tendency for rCBF in the left posterior cingulate gyrus and left middle frontal gyrus to be lower at Ex2 than at Rest ($P<0.01$, uncorrected).

Quantitative Analysis

Quantitative results for gCBF are shown in Table 3 and Figure 3B. Global CBF was 27.9% higher at Ex1 (67.2 ± 20.6 mL/100 g per minute) than at Rest (52.5 ± 10.5 mL/100 g per minute), but gCBF at Rest was similar to the level at Ex2 (53.0 ± 8.9 mL/100 g per minute). Among individual subjects (Figure 3B), gCBF ranged from 32.7 to 64.0, from 40.8 to 105.8, and from 40.8 to 69.1 mL/100 g per minute at Rest, Ex1, and Ex2, respectively. In one subject, gCBF was lower at both Ex1 and Ex2 than at Rest, and in another subject, gCBF did not change between Rest and Ex1 but was lower at Ex2. In the other eight subjects, gCBF was higher at Ex1 than at Rest and was lower at Ex2 than at Ex1.

Using the SPM results, we next selected ROIs for analysis of the 5-mm-thick normalized MRIs, which were averaged across all the subjects (Figure 2). The rCBF values in the individual ROIs were calculated from the corresponding normalized PET images, which were co-registered to the 5-mm-thick MRIs. Quantitative data for the ROIs are shown in Table 3. In this analysis, rCBF was increased at both Ex1 and Ex2 in the $M1_{Leg}$, $S1_{Leg}$, and cerebellar vermis. In those areas, rCBF was 50.0% to 70.5% higher at Ex1 than at Rest, and was 25.9% to 40.1% higher at Ex2 than at Rest. In the SMA, cerebellar hemisphere (inferior) and insular cortex, rCBF was increased only at Ex1. In those areas, rCBF was 32.3% to 50.5% higher at Ex1 than at Rest.

Table 2. Brain regions showing significantly higher rCBF at Ex1 and Ex2 than at Rest

A. Increased rCBF at Ex1 versus Rest

Region (Brodmann area)	*MNI (x, y, z)*	*Voxel number*	*Z-score*
Cerebellar vermis	2, −52, −18	73	4.18*
Sensorimotor cortex	0, −24, 62	73	4.11*
Supplementary motor area	0, −12, 64	104	3.67
Right cerebellum hemisphere	20, −52, −56	296	3.61
Left cerebellum hemisphere	−28, −56, −46	215	3.67
Left insula cortex	−34, 4, 6	224	3.34

B. Increased rCBF at Ex2 versus Rest

Region (Brodmann area)	*MNI (x, y, z)*	*Voxel number*	*Z-score*
Cerebellar vermis	2, −50, −20	37	4.93*
Sensorimotor cortex	−4, −24, 64	125	4.22
Supplementary motor area	0, −18, 64	43	3.57

MNI, Montreal Neurological Institute; rCBF, regional cerebral blood flow; ROIs, regions of interest. The brain regions listed showed significant increases in rCBF to $P<0.05$ (corrected), or to $P<0.001$ (uncorrected) in ROIs within regions selected *a priori* based on earlier findings. Within regions selected *a priori*, a small volume correction was applied. MNI (*x, y, z*), Montreal Neurological Institute coordinates of maximally increased voxels. The number of voxels per cluster is given (total search volume, 237,778 voxels). *Significance surviving correction for multiple comparisons.

DISCUSSION

Increased Regional Cerebral Blood Flow in Motor-Related Regions during Dynamic Exercise

The primary finding of this investigation was that rCBF is prominently increased in the $M1_{Leg}$, $S1_{Leg}$, SMA, cerebellar vermis, cerebellar hemispheres, and left insula cortex during the initial phase of exercise, but that increase was attenuated at later times during the exercise. Similarly, Christensen *et al*[7] also measured rCBF during a cycling exercise using PET and showed rCBF to be increased in the $M1_{Leg}$, $S1_{Leg}$, SMA, and vermis. In that study, however, the rCBF voxel counts were normalized to an intracranial mean of 100 in subjects at Rest and during active cycling. Absolute changes in rCBF between rest and exercise, such as those reported here, were not reported. Furthermore, both the timing of the rCBF measurements and the exercise intensity differed between the two studies. In the earlier study, a single PET scan was acquired over 1 minute beginning 10 seconds after the Ex1. In the present study, we acquired two scans over 2 minutes beginning 3 minutes and 13 minutes after the Ex1. In addition, although a constant load cycling exercise with a cadence of 60 r.p.m. was reported in the earlier study, the workload was not described. Several studies have employed PET to investigate the functional neuroanatomy of central command in the context of exercise.[11,12] In those studies,

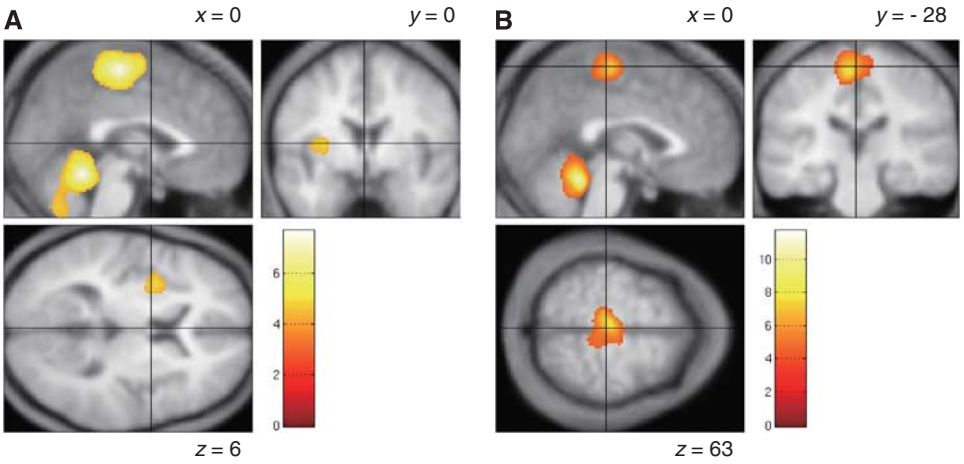

Figure 4. Brain regions showing higher regional cerebral blood flow at Ex1 (**A**) and Ex2 (**B**) than at Rest. Areas of significant common activation above $P<0.001$ are color-scaled according to the *T* score (scale given in the Figure). Group data are presented on an averaged T1-weighted structural image derived from the 10 subjects and normalized to the Montreal Neurological Institute (MNI) standard space. Montreal Neurological Institute coordinates in the *x* dimension and *y* dimension are given for parasagittal and coronal slices, respectively.

Table 3. Changes in global and regional cerebral blood flow from rest to exercise

Region	*Side*	*Volume (mL)*	*CBF (mL /100 g per minute)*			*Proportional changes (%)*		
			Rest	*Ex1*	*Ex2*	*Ex1 (From Rest)*	*Ex2 (From Rest)*	*Ex2 (From Ex1)*
Global CBF	—	1019	52.5 ± 10.5	67.2 ± 20.6**	53.0 ± 8.9†	27.9 ± 28.6	2.6 ± 13.5	− 17.2 ± 15.2
Regions where rCBF was higher at both Ex1 and Ex2 than at Rest								
Primary sensorimotor cortex	Right	4.7	57.6 ± 11.8	97.6 ± 29.9***	79.6 ± 20.2**,†	68.8 ± 35.4	39.7 ± 28.6	− 15.6 ± 14.9
	Left	4.7	57.2 ± 12.9	97.5 ± 29.6***	78.6 ± 17.8**,†	70.5 ± 35.0	40.1 ± 27.9	− 16.1 ± 15.3
Vermis	—	3.1	62.7 ± 12.7	94.7 ± 27.4***	78.1 ± 15.3*,†	50.0 ± 25.6	25.9 ± 15.6	− 14.5 ± 13.5
Regions where rCBF at Ex1 but not Ex2 was higher than at Rest								
Supplementary motor area	Right	2.0	63.5 ± 14.1	95.2 ± 28.9***	76.3 ± 17.3†	50.5 ± 33.3	22.8 ± 25.0	− 16.7 ± 14.3
	Left	2.0	63.2 ± 14.4	93.7 ± 28.0***	74.2 ± 18.1††	49.2 ± 31.5	20.1 ± 26.2	− 17.8 ± 15.9
Cerebellum (inferior)	Right	1.6	62.7 ± 14.5	86.4 ± 24.7***	70.7 ± 14.9†	38.3 ± 26.6	15.6 ± 23.6	− 15.2 ± 14.8
	Left	1.6	64.7 ± 15.5	88.8 ± 26.0***	70.6 ± 14.0††	37.5 ± 25.6	11.2 ± 16.3	− 17.3 ± 14.3
Insula cortex	Right	3.1	58.6 ± 12.9	77.5 ± 24.7**	63.2 ± 10.5†	32.3 ± 28.6	10.5 ± 20.0	− 14.1 ± 17.2
	Left	3.1	58.5 ± 13.0	80.8 ± 24.8***	64.0 ± 13.2††	37.6 ± 25.6	10.8 ± 14.7	− 17.6 ± 14.5

Values are shown as mean ± s.d. ($n=10$). Significance of difference from Rest: *$P<0.05$, **$P<0.01$, ***$P<0.001$. Significance of difference from Ex1: $^{\dagger}P<0.05$, $^{\dagger\dagger}P<0.01$.

however, rCBF measurements were made during isometric or handgrip exercise instead of dynamic exercise and were normalized to global mean of 50 mL/100 g per minute instead of using absolute values. In addition, while earlier SPECT studies demonstrated changes in rCBF during cycling ergometer exercise, they did not provide absolute values of rCBF.[8,9] Moreover, in contrast to PET-measured CBF, which is calculated on Fick's principle, linearity of SPECT-measured CBF to the true CBF may not be guaranteed in exercise condition. Thus, in contrast to the earlier studies, we were able to quantitatively analyze for the first time rCBF at both the initial phase and at a later phase of a steady-state cycling exercise.

In the $M1_{Leg}$, $S1_{Leg}$, and SMA, three areas where rCBF was higher at Ex1 than at Rest, the size of areas showing changes in rCBF appeared to be similar to those reported previously.[7] In the SMA, moreover, the area showing increased rCBF at Ex1 was larger than at Ex2, indicating that the area of the increased rCBF had declined by Ex2 (Table 2, Figure 4). Similarly, the relative increase in rCBF in the $M1_{Leg}$ and $S1_{Leg}$ differed considerably between the Ex1 and Ex2 (70% versus 39%), despite the constant VO_2. The lack of change in VO_2 is an indirect indicator of unchanging afferent input from the working muscles and implies the presence of a mechanism specifically regulating rCBF during the onset phase of exercise. The reduction in the magnitude of the increase in rCBF in the SMA between the Ex1 and Ex2 appears to correspond to the anatomic difference between the SMA proper and the preSMA (Figure 4).[19,20] It has been suggested that activation in the SMA proper is associated with less complex components of a task, whereas activation in the preSMA is associated with more complex components.[20] In that context, our finding that involvement of the SMA diminished over the time course of the exercise might be indicative of adaptation to the exercise, which would be manifested as a sensation of greater effort during the initial phase of exercise than during the later phase.

Earlier imaging studies of cycling exercise reported increases in rCBF in the cerebellar vermis.[7,8,11] In the present study, we observed exercise-related increases in rCBF in the cerebellar vermis and hemispheres. This is likely attributable to the role of

the cerebellum in motor control, as well as the anatomic connectivity between the cerebellar vermis and the working muscles via the spinocerebellar tract, and between the cerebellar hemispheres and the sensorimotor cortex via the pontocerebellar and corticopontine tracts. In addition to its role in motor control, the cerebellum is also involved in autonomic nervous function, and several studies have demonstrated that some modules within the cerebellum are dedicated to cardiovascular function and exert influence on the brainstem cardiovascular centers.[21,22] For example, anatomic evidence supports the involvement of fastigial nucleus neurons and the medial portion of the cerebellar vermis in cardiovascular function.[23,24] In the present study, areas of the cerebellar vermis showing increased rCBF corresponded to the medial portion of the vermis, including the fastigial nucleus. It is noteworthy, that the vermis is the only cerebellar region in which distinct increases in rCBF were identified at both Ex1 and Ex2. By contrast, the increases in rCBF seen in the cerebellar hemispheres at Ex1 were abolished by Ex2 (Table 2, Figure 4). Taking into consideration the hemodynamic changes that occur during exercise, it is tempting to speculate that the relationship between the sensorimotor cortex and insular cortex might corresponds to that between the vermis and the cerebellar hemispheres.

Physiologic Factors and Changes in Cerebral Blood Flow

At Rest, gCBF ranged from 32.7 to 64.0 mL/100 g per minute (Figure 3B). Considering that the lower P_aCO_2 values would affect gCBF, the observed gCBF values are consistent with the normal database in the Tokyo Metropolitan Institute of Gerontology. Although the individual intensities of cycling exercise were determined such that $\dot{V}O_2$ kinetics would attain a steady state, and each subject had nearly the same $\dot{V}O_2$ between Ex1 and Ex2, our finding that the $\dot{V}O_2$ plateau at Ex2 varied from 12.1 to 25.5 mL/minute is suggestive of the heterogeneity of the exercise intensity among the subjects (Table 1, Figure 3A). As a result, the patterns of change in P_aCO_2 between Ex1 and Ex2 differed among individual subjects, which would affect gCBF. Considered as a group, however, our data demonstrate that P_aCO_2 did not change and gCBF declined between Ex1 and Ex2, which was confirmed by repeated measures one-way analysis of variance.

From Rest to Ex1, rCBF increased in parallel with the physiologic parameters, including CO and $\dot{V}O_2$. Considering that some brain regions would be involved in autonomic regulation,[16,25,26] the response of the cardiovascular system to exercise might be associated with changes in rCBF. However, we did not investigate the association between changes in discrete regions and changes in physiologic parameters. However, our finding that gCBF had increased by 27.9% at Ex1 with no change in MBP implies that MBP is not the single factor determining rCBF, as has been suggested.[1,3] About the relationship between blood pressure and CBF, cerebral autoregulation has been shown to keep CBF stable at MBPs ranging from 60 to 150 mm Hg.[27] More specifically, static cerebral autoregulation governs CBF during gradual, progressive changes in cerebral perfusion,[27] whereas dynamic cerebral autoregulation modulates CBF in response to more rapid changes in the arterial blood pressure that occur on a time scale measured in seconds.[28] Such dynamic cerebral autoregulation functions at the onset of static exercise in parallel with a rapid increase in MBP evoked by a Valsalva-like maneuver.[29] Notably, our results demonstrate that an increase in gCBF occurs during the initial phase of dynamic exercise without either an elevation of MBP or a Valsalva-like maneuver, such as that seen during static exercise. Thus, although dynamic cerebral autoregulation could not be examined in the present study owing to the insufficient temporal resolution of the modality used, the regulatory mechanism governing the changes in gCBF between Rest and Ex1 could not be related to a change in MBP or a Valsalva-like maneuver at the initiation of the exercise.

In addition to cerebral autoregulation, P_aCO_2 is a major contributor to changes in rCBF via vasodilatation or constriction.[30] However, the small increase of 2 mm Hg in P_aCO_2 seen in the present study would not be sufficient to account for the increases in rCBF seen at both Ex1 and Ex2 ($\sim$70.5% and $\sim$40.1%, respectively), even taking the heterogeneous nature of the brain regions involved in the cerebrovascular response to CO_2 into consideration.[31] Consequently, neural control in large regions of the brain may be required to initiate dynamic exercise and could account for the large increase in rCBF and gCBF, which are beyond the range of the cerebrovascular response to CO_2. The finding that gCBF at Ex2 was not higher than at Rest, despite a 2-mm Hg increase in P_aCO_2, also implies that a mechanism other than the cerebrovascular response to CO_2 has a role in regulating gCBF later during dynamic exercise. Given that our SPM analysis demonstrated that there was a tendency for rCBF to decline in some regions (e.g., left posterior cingulate gyrus and left middle frontal gyrus), these reductions could account for the lower gCBF at Ex2. We speculate that the reductions in gCBF later during dynamic exercise offset the effect of the cerebrovascular response to CO_2. Furthermore, because the dynamic exercise continued for 13 minutes and P_aCO_2 was sustained at a higher level than at Rest throughout, no information is provided regarding the duration for which the increase in CBF can be sustained after the cerebrovascular response to CO_2 is applied. Cerebrovascular response to CO_2 is defined using several steps of the relationships between P_aCO_2 and CBF, but the duration of the steady-state hypercapnia in those studies was 5 minutes, at most.[32] Thus, the finding that gCBF did not differ between Ex2 and Rest, despite the increase in P_aCO_2, cannot be solely based on the conventional cerebrovascular response to CO_2.

During moderate steady-state dynamic exercise, gCBF increases at the initial phase in parallel with $\dot{V}O_2$ and CO kinetics and subsequently declines, despite the lack of change in the physiologic parameters other than CO, which increased slightly. Given that CO is a possible influencing factor for regulating CBF although the mechanism have not been clearly delineated,[5,32,33] our data suggest an effect of changes in CO on CBF.

When considering the mechanism by which CBF is regulated during dynamic exercise from the perspective of cerebral autoregulation and the cerebrovascular response to CO_2, it should be recognized that these classic mechanisms were applied in a static situation in which other factors related to exercise (e.g., CO) were held constant. Our findings suggest the possibility that during dynamic exercise, which involves changes in several physiologic parameters, factors other than blood pressure and CO_2, may be affecting the regulation of CBF.[32]

Central Command and Interoceptive Stimuli

During the cardiovascular response to exercise, signals from higher cortical centers (central command) and afferent input arising from the working muscles are integrated in the medulla.[34] Williamson *et al*[35] proposed to redefine central command as a network of higher brain structures capable of interpreting an individual's sense of effort and making appropriate autonomic adjustments. Two specific findings of the present study appear to be associated with central command. First, the increases in rCBF affected broad regions at Ex1 but not Ex2. Although we did not inquire about the subjects' ratings of perceived exertion during exercise, our impression is that the sense of effort was relatively low with the moderate exercise used in this study. But considering that the subjects likely adapted to the exercise over time, we would expect the sense of effort to have been higher at Ex1 than at Ex2. Second, the regions of increased rCBF (Tables 2 and 3) were consistent with the cortical regions thought most likely to be involved in central command. These regions include the insular cortex and anterior cingulate cortex,[8,9,11,12,36] which have a key

role in autonomic responses to sensory input reporting on physiologic conditions throughout the entire body.[16,25,37,38]

We found that the increase of rCBF in the left anterior insular cortex was more significant than in the right anterior insular cortex. This is in contrast to Christensen *et al*,[7] who did not observe an increase in rCBF in the insular cortex during a cycling exercise. This discrepancy is attributable to the difference between our analysis of absolute changes in rCBF, as compared with the use of a normalized intracranial mean.[7] Our SPM analysis revealed rCBF to be increased in the left anterior insular cortex ($P < 0.001$, uncorrected, Table 2 and Figure 4) but not in the right cortex. This lateralized increase of rCBF in the insular cortex is consistent with the previous SPECT study, which entailed light cycling exercise at a constant workload such that HR was no greater than 100 b.p.m. and MBP did not change.[8] Previous studies suggest the right insular cortex may be more closely associated with sympathetic activity, whereas the left insular may be more related to parasympathetic activity.[8,16,17] In that regard, Robinson *et al*[39] demonstrated that initial HR elevations during exercise, up to ~100 b.p.m., are due primary to vagal withdrawal—i.e., reduction of parasympathetic drive to the sinoatrial node. Further increases in HR primarily reflect an increase in sympathetic drive.[39,40] Considering that HR had increased to 96 b.p.m. at Ex1 and to 104 b.p.m. at Ex2, the exercise intensity used in the present study appears consistent with the concept of lateralization of autonomic control between the right and left insular cortices.

A recent review of the functional anatomy of interoceptive (visceral) stimuli described a pathway from the peripheral tissues to the anterior insular cortex and anterior cingulated cortex and argued that these interoceptive stimuli include awareness of body movement during exercise.[37,38] The role of the left insular cortex in the context of this pathway was apparent in the present study. From Rest to Ex1, $\dot{V}O_2$ increased owing to the enhanced oxygen utilization within the working muscles, and rCBF in the left insular cortex increased concomitantly. However, $\dot{V}O_2$ did not change between Ex1 and Ex2 because of to the stability of the conditions within the working muscles, and rCBF in the left insular cortex declined.

CONCLUSION

In summary, the present study demonstrated quantitative changes in rCBF at both the Ex1 and at a later phase during a steady-state cycling exercise. Our findings indicate that during the onset phase, gCBF increases although MBP does not, and the increases in rCBF in the $M1_{Leg}$, $S1_{Leg}$, SMA, cerebellum, and left insular cortex could be associated with the central command network as well as afferent inputs from the working muscles. Despite the lack of change in the cardiovascular response during the prolonged exercise, the initial increase in rCBF over large areas was transient, and gCBF returned to the resting level. Thus, rCBF appears to change during exercise, even when the cardiovascular response does not. Our results imply that the mechanism regulating rCBF at the Ex1 may differ from the mechanism regulating rCBF later during exercise. Further investigation will be needed to define the regulatory mechanism specific to the Ex1 and the relationship between the cardiovascular response and rCBF.

DISCLOSURE/CONFLICT OF INTEREST

The authors declare no conflict of interest.

ACKNOWLEDGMENTS

The authors thank Mr Kunpei Hayashi and Ms. Hatsumi Endo for their technical assistance.

REFERENCES

1 Ide K, Secher NH. Cerebral blood flow and metabolism during exercise. *Prog Neurobiol* 2000; **61**: 397–414.
2 Querido JS, Sheel AW. Regulation of cerebral blood flow during exercise. *Sports Med* 2007; **37**: 765–782.
3 Secher NH, Seifert T, Van Lieshout JJ. Cerebral blood flow and metabolism during exercise: implications for fatigue. *J Appl Physiol* 2008; **104**: 306–314.
4 Hellstrom G, Fischer-Colbrie W, Wahlgren NG, Jogestrand T. Carotid artery blood flow and middle cerebral artery blood flow velocity during physical exercise. *J Appl Physiol* 1996; **81**: 413–418.
5 Ide K, Horn A, Secher NH. Cerebral metabolic response to submaximal exercise. *J Appl Physiol* 1999; **87**: 1604–1608.
6 Linkis P, Jorgensen LG, Olesen HL, Madsen PL, Lassen NA, Secher NH. Dynamic exercise enhances regional cerebral artery mean flow velocity. *J Appl Physiol* 1995; **78**: 12–16.
7 Christensen LO, Johannsen P, Sinkjaer T, Petersen N, Pyndt HS, Nielsen JB. Cerebral activation during bicycle movements in man. *Exp Brain Res* 2000; **135**: 66–72.
8 Williamson JW, McColl R, Mathews D, Ginsburg M, Mitchell JH. Activation of the insular cortex is affected by the intensity of exercise. *J Appl Physiol* 1999; **87**: 1213–1219.
9 Williamson JW, McColl R, Mathews D, Mitchell JH, Raven PB, Morgan WP. Hypnotic manipulation of effort sense during dynamic exercise: cardiovascular responses and brain activation. *J Appl Physiol* 2001; **90**: 1392–1399.
10 Goodwin GM, McCloskey DI, Mitchell JH. Cardiovascular and respiratory responses to changes in central command during isometric exercise at constant muscle tension. *J Physiol* 1972; **226**: 173–190.
11 Critchley HD, Corfield DR, Chandler MP, Mathias CJ, Dolan RJ. Cerebral correlates of autonomic cardiovascular arousal: a functional neuroimaging investigation in humans. *J Physiol* 2000; **523**(Pt 1): 259–270.
12 Nowak M, Holm S, Biering-Sorensen F, Secher NH, Friberg L. 'Central command' and insular activation during attempted foot lifting in paraplegic humans. *Hum Brain Mapp* 2005; **25**: 259–265.
13 Whipp BJ. The slow component of O2 uptake kinetics during heavy exercise. *Med Sci Sports Exerc* 1994; **26**: 1319–1326.
14 Herscovitch P, Markham J, Raichle ME. Brain blood flow measured with intravenous H2(15)O. I. Theory and error analysis. *J Nucl Med* 1983; **24**: 782–789.
15 Raichle ME, Martin WR, Herscovitch P, Mintun MA, Markham J. Brain blood flow measured with intravenous H2(15)O. II. Implementation and validation. *J Nucl Med* 1983; **24**: 790–798.
16 Oppenheimer SM, Gelb A, Girvin JP, Hachinski VC. Cardiovascular effects of human insular cortex stimulation. *Neurology* 1992; **42**: 1727–1732.
17 Sander D, Klingelhofer J. Changes of circadian blood pressure patterns and cardiovascular parameters indicate lateralization of sympathetic activation following hemispheric brain infarction. *J Neurol* 1995; **242**: 313–318.
18 Jones NL, Robertson DG, Kane JW. Difference between end-tidal and arterial PCO2 in exercise. *J Appl Physiol* 1979; **47**: 954–960.
19 Nachev P, Kennard C, Husain M. Functional role of the supplementary and pre-supplementary motor areas. *Nat Rev Neurosci* 2008; **9**: 856–869.
20 Picard N, Strick PL. Motor areas of the medial wall: a review of their location and functional activation. *Cereb Cortex* 1996; **6**: 342–353.
21 Nisimaru N. Cardiovascular modules in the cerebellum. *Jpn J Physiol* 2004; **54**: 431–448.
22 Spyer KM. Central nervous control of the cardiovascular system. In: Mathias CJ, Bannister R (eds) *A Textbook of Clinical Disorders of the Autonomic Nervous Sysytem*. Oxford University Press: Oxford, UK, 1999, pp 45–55.
23 Bradley DJ, Paton JF, Spyer KM. Cardiovascular responses evoked from the fastigial region of the cerebellum in anaesthetized and decerebrate rabbits. *J Physiol* 1987; **392**: 475–491.
24 Supple Jr. WF, Kapp BS. Anatomical and physiological relationships between the anterior cerebellar vermis and the pontine parabrachial nucleus in the rabbit. *Brain Res Bull* 1994; **33**: 561–574.
25 Cechetto DF. Role of the cerebral cortex in autonomic function. In: Loewy AD, Spyer KM (eds). *Central Regulation of Autonomic Functions*. Oxford University Press: New York, NY, 1990, pp 208–223.
26 Saper CB. The central autonomic nervous system: conscious visceral perception and autonomic pattern generation. *Annu Rev Neurosci* 2002; **25**: 433–469.
27 Paulson OB, Strandgaard S, Edvinsson L. Cerebral autoregulation. *Cerebrovasc Brain Metab Rev* 1990; **2**: 161–192.
28 Zhang R, Zuckerman JH, Iwasaki K, Wilson TE, Crandall CG, Levine BD. Autonomic neural control of dynamic cerebral autoregulation in humans. *Circulation* 2002; **106**: 1814–1820.
29 Pott F, Van Lieshout JJ, Ide K, Madsen P, Secher NH. Middle cerebral artery blood velocity during intense static exercise is dominated by a Valsalva maneuver. *J Appl Physiol* 2003; **94**: 1335–1344.
30 Lassen NA. Cerebral blood flow and oxygen consumption in man. *Physiol Rev* 1959; **39**: 183–238.

31 Ito H, Yokoyama I, Iida H, Kinoshita T, Hatazawa J, Shimosegawa E *et al*. Regional differences in cerebral vascular response to PaCO2 changes in humans measured by positron emission tomography. *J Cereb Blood Flow Metab* 2000; **20**: 1264–1270.
32 Ainslie PN, Duffin J. Integration of cerebrovascular CO2 reactivity and chemoreflex control of breathing: mechanisms of regulation, measurement, and interpretation. *Am J Physiol Regul Integ Comp Physiol* 2009; **296**: R1473–R1495.
33 Gonzalez-Alonso J, Dalsgaard MK, Osada T, Volianitis S, Dawson EA, Yoshiga CC *et al*. Brain and central haemodynamics and oxygenation during maximal exercise in humans. *J Physiol* 2004; **557**: 331–342.
34 Waldrop TG. Central neural contrpl of respiration and circulation during exercise. In: Rowell LB, Shepherd JT (eds) *Handbook of Physiology, chapter 9, section 12, Exercise: Regulation and Integration of Multiple Systems*. American Physiology Society: Bethesda, MD, 1996, pp 333–380.
35 Williamson JW, Fadel PJ, Mitchell JH. New insights into central cardiovascular control during exercise in humans: a central command update. *Exp Physiol* 2006; **91**: 51–58.
36 King AB, Menon RS, Hachinski V, Cechetto DF. Human forebrain activation by visceral stimuli. *J Comp Neurol* 1999; **413**: 572–582.
37 Craig AD. How do you feel? Interoception: the sense of the physiological condition of the body. *Nat Rev Neurosci* 2002; **3**: 655–666.
38 Craig AD. How do you feel--now? The anterior insula and human awareness. *Nat Rev Neurosci* 2009; **10**: 59–70.
39 Robinson BF, Epstein SE, Beiser GD, Braunwald E. Control of heart rate by the autonomic nervous system. Studies in man on the interrelation between baroreceptor mechanisms and exercise. *Circ Res* 1966; **19**: 400–411.
40 Billman GE, Dujardin JP. Dynamic changes in cardiac vagal tone as measured by time-series analysis. *Am J Physiol* 1990; **258**: H896–H902.